

Empirical Mode Decomposition and Wavelet Decomposition in Respiratory Sounds Processing

Chengwei Han (✉ by2003104@buaa.edu.cn)

Beihang University <https://orcid.org/0000-0003-0980-0584>

Yixuan Wang

Beihang University

Zhibo Sun

Beihang University

Xie Fei

Chinese PLA General Hospital

Research

Keywords: Empirical Mode Decomposition, Wavelet Decomposition, Spectrum Subtraction, Hilbert Transform

Posted Date: February 16th, 2023

DOI: <https://doi.org/10.21203/rs.3.rs-2549152/v1>

License:   This work is licensed under a Creative Commons Attribution 4.0 International License.

[Read Full License](#)

2 Empirical Mode Decomposition and Wavelet Decomposition 3 in Respiratory Sounds Processing

4 Chengwei Han ¹, Yixuan Wang ¹, Shuai Ren ¹, Na Wang ², Zhibo Sun ², Fei Meng ¹, Xuelin
5 Zhao ³, Jianwei Wang ⁴ and Fei Xie ^{5,*}

6 ¹ School of Automation Science and Electrical Engineering, Beihang University

7 ² Engineering Training center, Beihang University, Beihang University

8 ³ Department of Orthopedics, Chinese PLA General Hospital

9 ⁴ Department of critical care medicine, Puyang people's Hospital of Henan Province

10 ⁵ Department of Pulmonary and Critical Care Medicine, Chinese PLA General Hospital

11 * Correspondence: hcwjhsuiao@163.com;

12

13 **Abstract:** In order to process respiratory sounds to achieve acquiring available information of
14 sound signals Empirical Mode Decomposition (EMD) and Wavelet Decomposition (WD) are
15 applied separately to analyze lung sound signals. The de-noise of original signals is processed
16 with spectral subtraction method. EMD divides the signal into independent Intrinsic Mode
17 Functions (IMFs). Moreover, WD method decomposes the signal with wavelet transform. After
18 receiving the decomposition signals of EMD and WD, a comparison is demonstrated.
19 According to the results, WD has 85% signal information concentrate on layer 7 and Hilbert
20 diagram shows the EMD owns more efficiency in decomposing signals with information
21 keeping.

22

23 **Key words:** Empirical Mode Decomposition; Wavelet Decomposition; Spectrum Subtraction;
24 Hilbert Transform.

25

26

27 1. Introduction

28 Recently, COVID-19 becomes a serious worldwide issue which is need to be fixed. This
29 virus leads to serious lung disease which is the reason many people passed in the past year. In
30 the procession of curing the lung disease to obtain the breathing information is extremely
31 significant. The respiratory sounds can demonstrate important lung information of patients.[1]
32 Thus, analyzing of respiratory sounds of patients to achieve getting the information is
33 significant.[2]-[3] This article is going to discuss about the decomposition methods of original
34 respiratory sound signals efficiency. The methods include Empirical Mode Decomposition
35 (EMD) and Wavelet decomposition.

36 After the acquisition of the respiratory sounds, the first step is to pre-process the signal.
37 Respiratory sounds are sounds of breathing within the lungs over the chest wall. [4] During
38 the period of breathing and acquisition of signal, the noise cannot be avoided. Moreover, the
39 lung is near to the heart. Thus, the heart sound is unpreventable noise, which can have severe
40 influence on acquisition of lung sound signals. [5]

41 There are many methods to de-noise the signals. Hadjileontiadis et al. demonstrated a
42 method that using the combination of fractal dimension (FD) and EMD eliminate the noise of

43 lung sound signals. [6] Emmanouilidou et al. [7] introduced adaptive subtraction method to
 44 decrease the heart sound noise of respiratory signal. Moreover, in 2021, Haider used Spectral
 45 Subtraction method with EMD and hurst to do the de-noise of lung sound signals, which is
 46 proved has excellent performance.[8] In this article, the method of Spectral Subtraction De-
 47 noise method is chosen to do the noise elimination.

48 Empirical mode decomposition was introduced in 1998 by N.E. Huang to process non-
 49 linear and unstable signals.[9] After EMD method coming out, a bunch of optimization
 50 algorithms and papers appeared based on the research result of N.E. Huang. [10] EMD
 51 algorithm has widely application category in medical area, and it can be used for analyzing
 52 lung sounds. [11]

53 According to the characteristics of Wavelet Transform (WT), mature and low-complexity,
 54 it has been widely used for processing respiratory sound signals. Hossain I et al proposed a
 55 method using WT combine with spectral characteristics to build filter of respiratory sounds
 56 signals. [12] In 2004, a method based on fast WT was used for lung sounds classification.[13]
 57 In this article, based on EMD and WD respiratory sound signals will be analyzed. The signal
 58 will be de-noise by spectrum subtraction method, then using EMD and WD to analyze the
 59 denoise signals separately. In the end, the efficiency of keeping the original signals
 60 characteristics will be compared.

61 For respiratory sound signals analyzing, signal information keeping is a significant
 62 problem. This paper is trying to compare EMD and WD to examine the ability of keeping
 63 original signal information. Firstly, this article chooses spectral subtraction de-noise method in
 64 pre-processing original signal. Secondly, the EMD method is demonstrated. Moreover, WD is
 65 used for signal decomposition and Shannon entropy of relative wavelet energy is used for
 66 texting.

67 2. Spectral Subtraction De-noise

68 In this paper, the de-noise method based on spectral subtraction was used to do the voice
 69 signal de-noise. First of all, assuming the voice sequence as $x(n)$ to do the window framing of
 70 $x(n)$. Thus, $x_i(m)$ can be got after window framing. Afterall, Discrete Fourier Transform
 71 method is used to deal with $x_i(m)$. The equation below can be achieved:

$$72 \quad x_i(k) = \sum_{m=0}^{N-1} x_i(m) e^{j\frac{2\pi mk}{N}} \quad k = 0, 1, 2, \dots, N-1 \quad (1)$$

73 Phase angle is obtained with equation (2)

$$74 \quad X_{angle}^i(k) = \arctan \left[\frac{Im(x_i(k))}{Re(x_i(k))} \right] \quad (2)$$

75 Then the energy of the noise is:

$$76 \quad D(k) = \frac{1}{NIS} \sum_{i=1}^{NIS} |X_i(k)|^2 \quad (3)$$

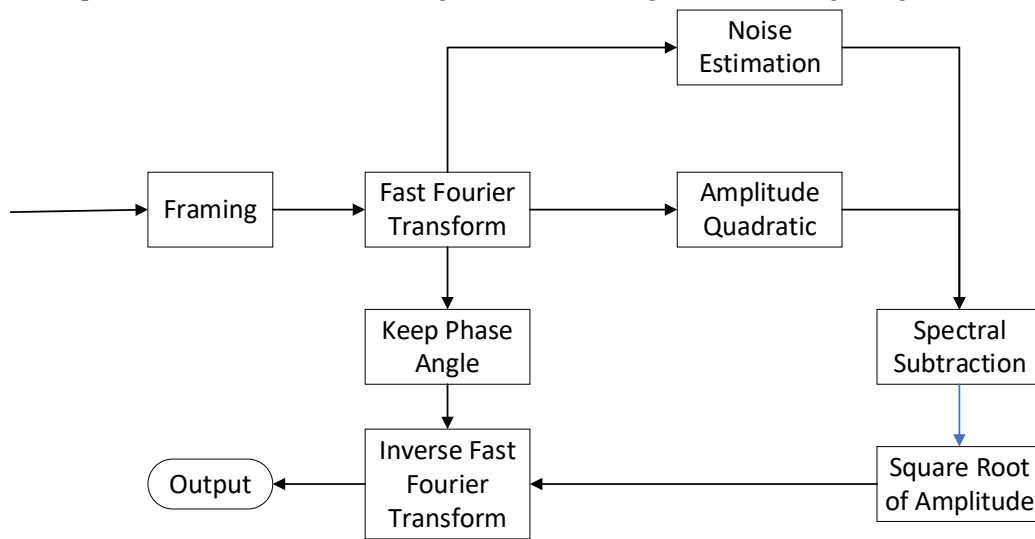
77

78 After all the steps above, the below equation can be used for de-noise:

$$79 \quad |x_i(k)|^2 = \begin{cases} |X_i(k)|^2 - a \times D(k) & |X_i(k)|^2 \geq a \times D(k) \\ b \times D(k) & |X_i(k)|^2 < a \times D(k) \end{cases} \quad (4)$$

80

The spectral subtraction de-noise algorithm block diagram is showing in figure 1.



81

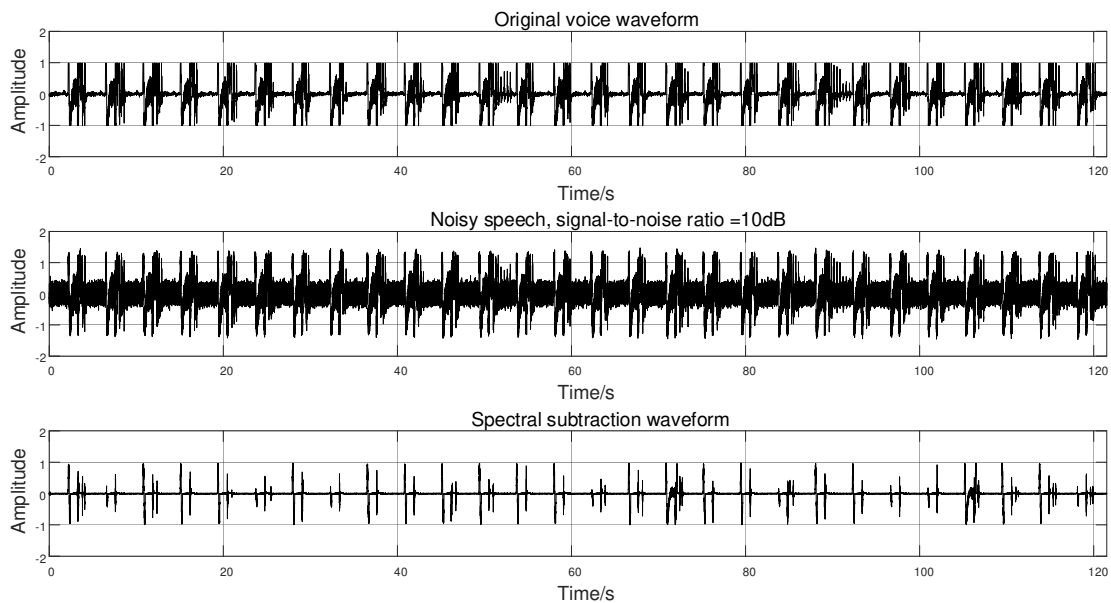
82

Figure 1. spectral subtraction de-noise block diagram

83

The de-noise result of the original signal is showing in Figure 2. As can be seen in the figure, with this de-noise method, the noise can be decreased efficiently, and the characteristics of the signals can be kept.

85



86

87

Figure 2. Spectral subtraction waveform comparison

88

As can be seen from figure 2, the spectrum can provide efficiently de-noise of the respiratory signal. After the denoise, the characteristics of the original signal are still kept. With the 10 DB signal to noise ratio (SNR), the proposed method can eliminate the noise contaminations very well. The respiratory sounds signals were started sampling at 4000 Hz rate. Afterall, let the result pass a Butterworth Band-pass filter of 20-2000Hz, which can eliminate all the high frequency noises. Moreover, the spectral subtraction was used to get further outcoming of the denoise of signals.

93

95

3. Empirical mode decomposition

96

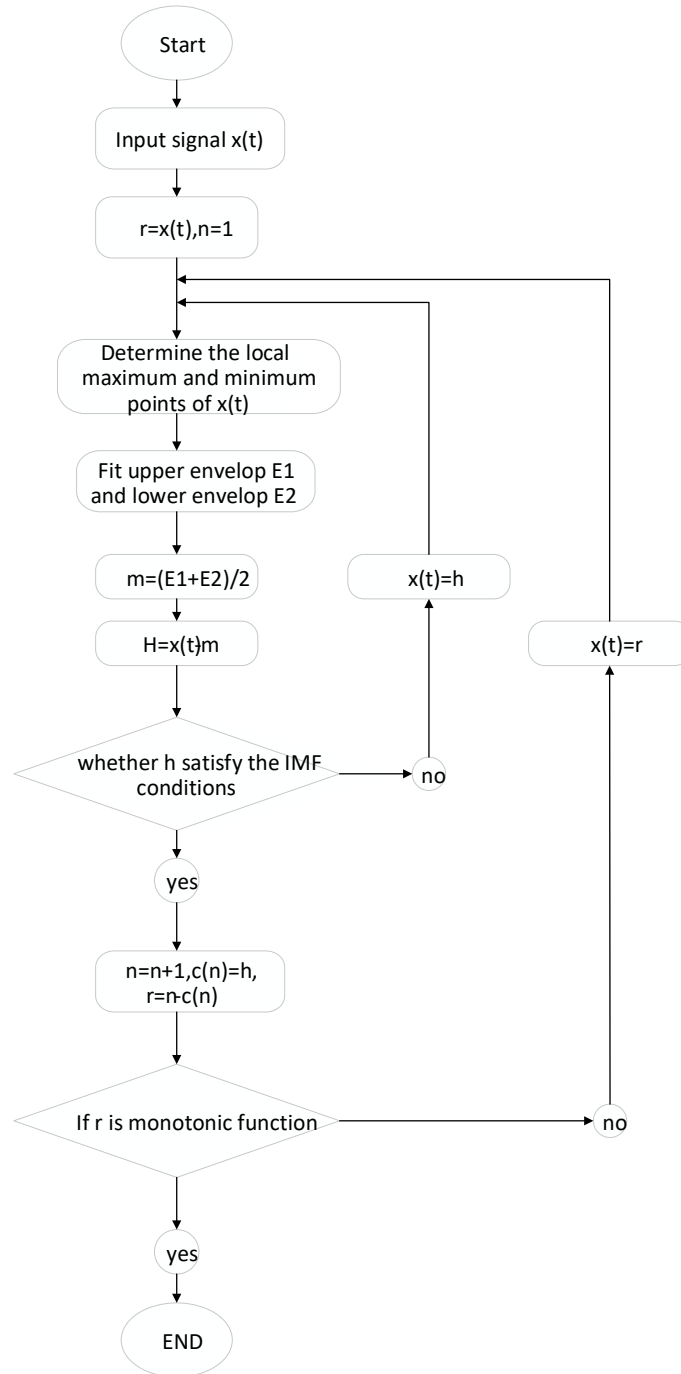
EMD method has advance in non-stationary and non-linear signals analysis. The

97 respiratory sound signal can be divided into several independent intrinsic mode functions
 98 (IMFs) based on frequency difference. [13]

99 To achieve the EMD analysis, the first step is to get the mean value of upper and lower
 100 envelop of input signal $x(t)$. Assuming the mean value as m_1 , the equation (5) below can be
 101 got:

$$h_1 = x(t) - m_1 \quad (5)$$

102 The second step is using h_1 as new $x(t)$ to run the process above again until h_1 satisfy
 103 the IMF conditions then output the first IMF as C_1 .
 104
 105



106

107

Figure 3. Empirical mode decomposition algorithm flowchart

108 With the separation of C_1 and $x(t)$, a signal r_1 without high-frequency components is
 109 obtained.

110
$$r_1 = x(t) - C_1 \tag{6}$$

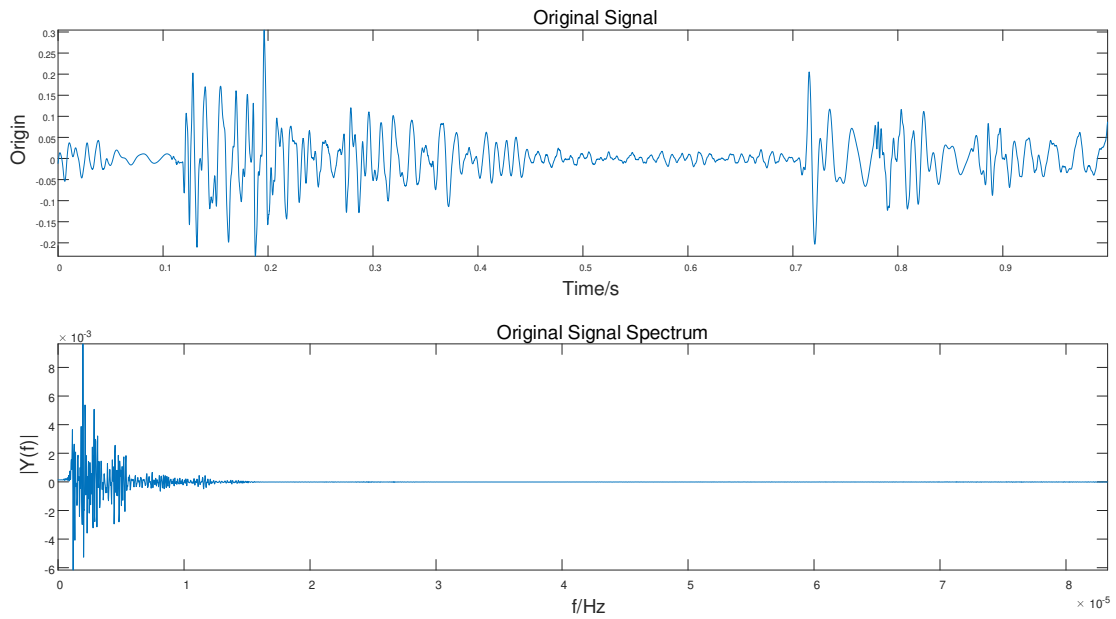
111 Repeat the steps above until the remain signal is monotonic function.

112
$$r_n = r_{n-1} - C_n \tag{7}$$

113 Overall, the original signal $x(t)$ can be represent as below:

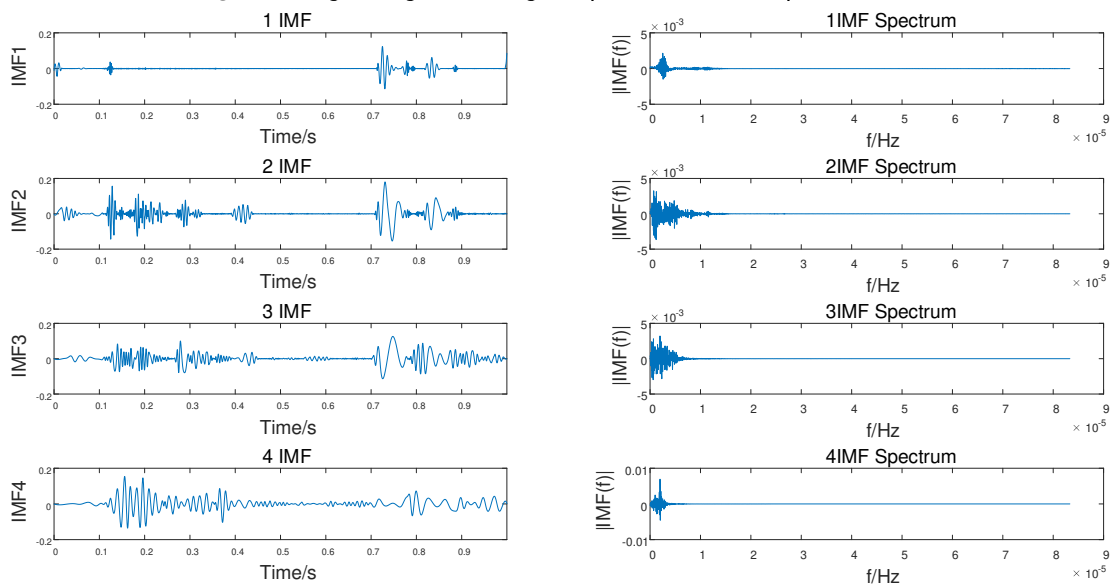
114
$$x(t) = \sum_{i=1}^n C_i(t) + r_n(t) \tag{8}$$

115 The whole algorithm flowchart of EMD is demonstrated in Figure 3.



116

Figure 4. original signal and signal spectrum of mild sputum stasis



117

118

Figure 5. IMF 1 to 4 of mild sputum stasis respiratory sound and spectrum

119

120

According to the method described above, the different signals were processed with EMD.

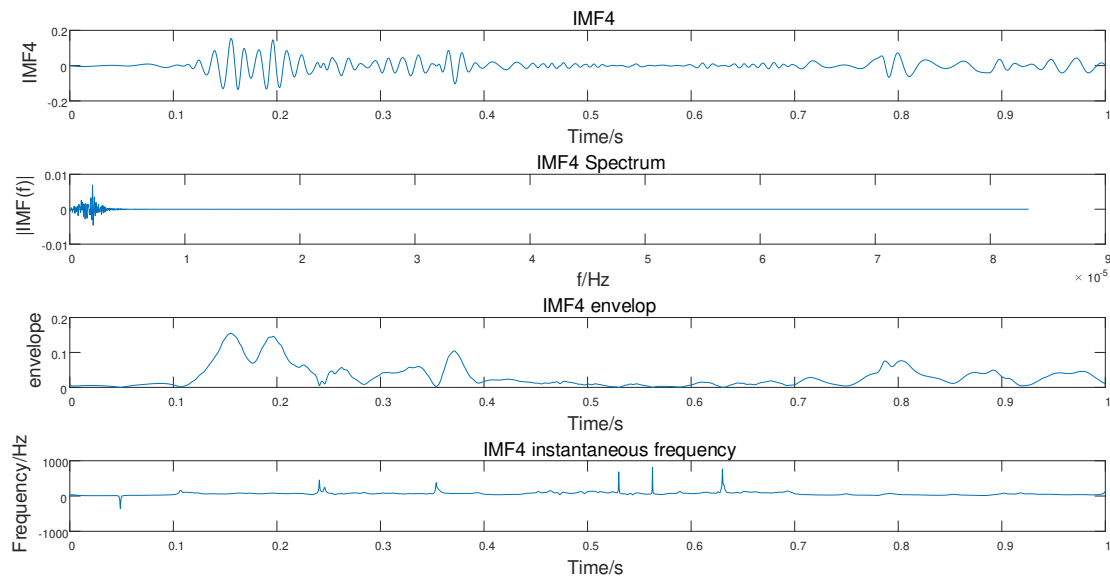
121

Figure 4 shows the original signal of mild sputum stasis respiratory lung sounds. The spectrum

122 of original signal is illustrated in Figure 4 as well.

123 According to the characteristics of EMD, the 1st to 4th IMFs are the independent
124 components with higher frequency than the rest. In this paper, only the first 4 IMFs results are
125 given. Based on figure 5, IMF 3 and 4 can reflect the characteristics of original signal most
126 effectively. Thus, the IMF 4 was chosen to illustrate the characteristics. Figure 6 is showing
127 the signal of IMF 4 and spectrum. Moreover, the envelope of IMF 4 and instantaneous frequency
128 are also given.

129 Figure 6 demonstrates that the mild sputum stasis respiratory sound has slight change in
130 instantaneous frequency change.



131

132

Figure 6. mild sputum stasis respiratory sound IMF 4 characteristics

133

134

135

136

137

138

In figure 7 and 8, the comparison of light severe and severe of sputum stasis can be made. As shown in the figures, the mild sputum stasis signal has regular breath signal with the longest period. The light severe sputum stasis signal shows that the breath become more hush and unregular. The severe sputum stasis original signal demonstrates that the more severe sputum stasis, the more unregular signal it is.

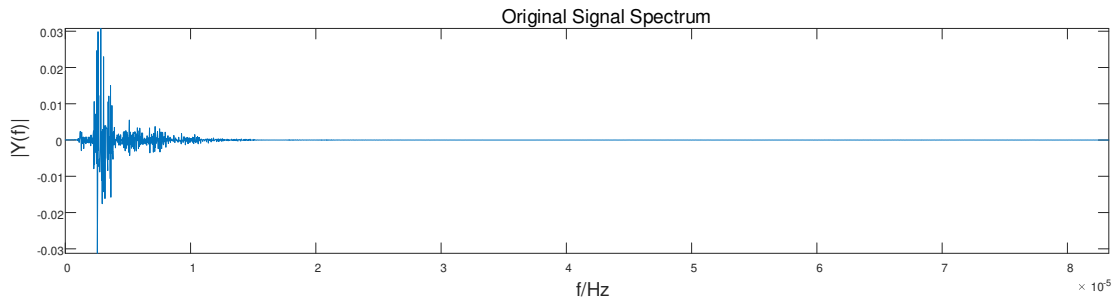
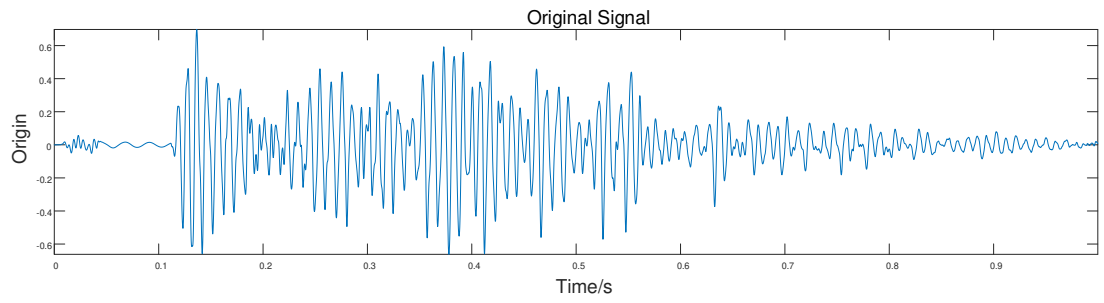


Figure 7. Original signal of light severe sputum stasis

139
140
141

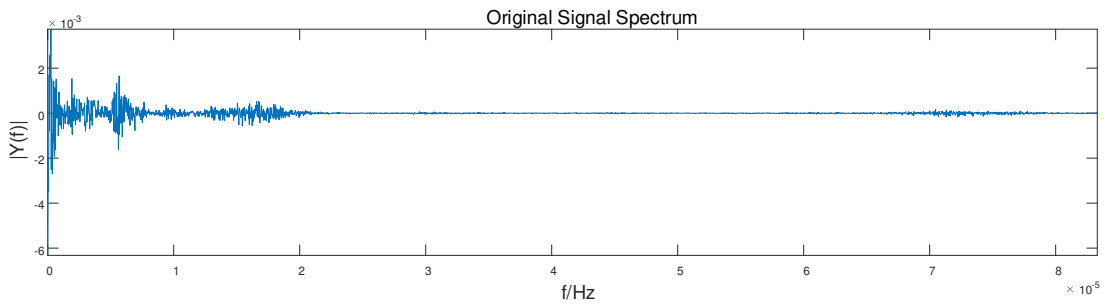
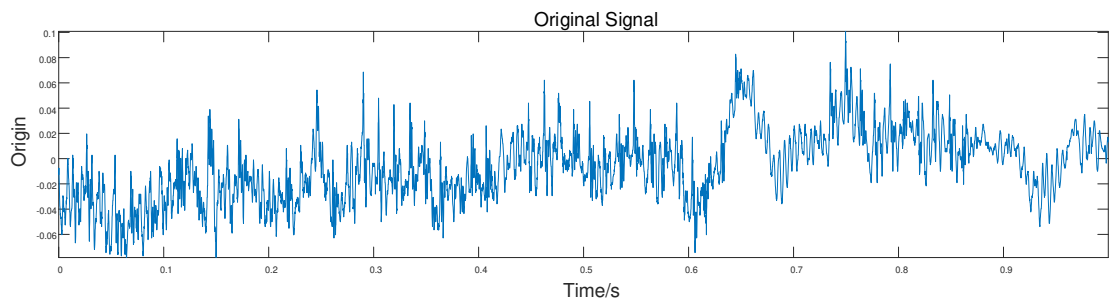
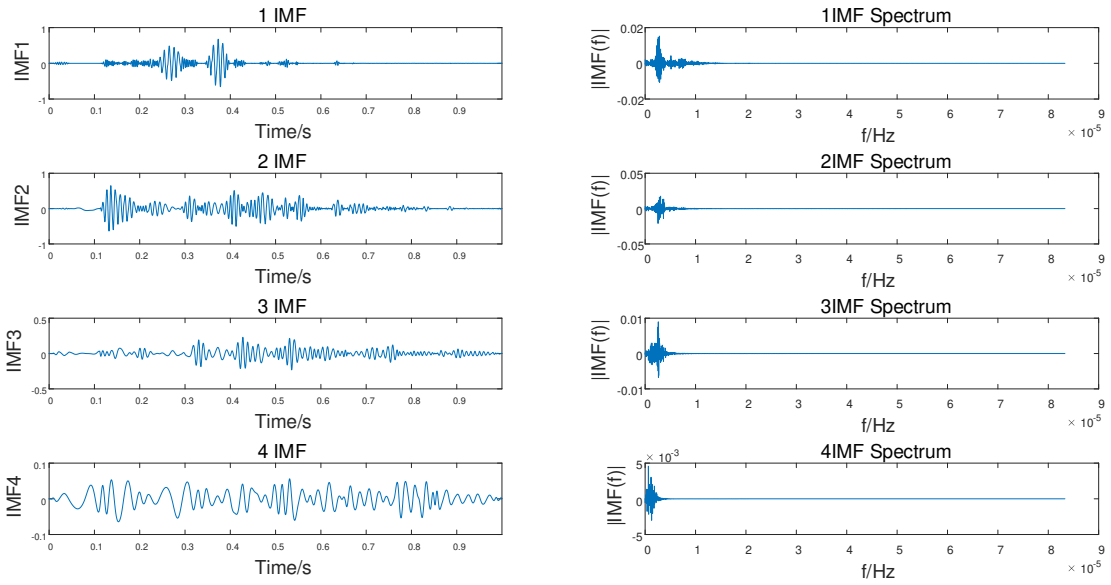


Figure 8. Original signal of severe sputum stasis

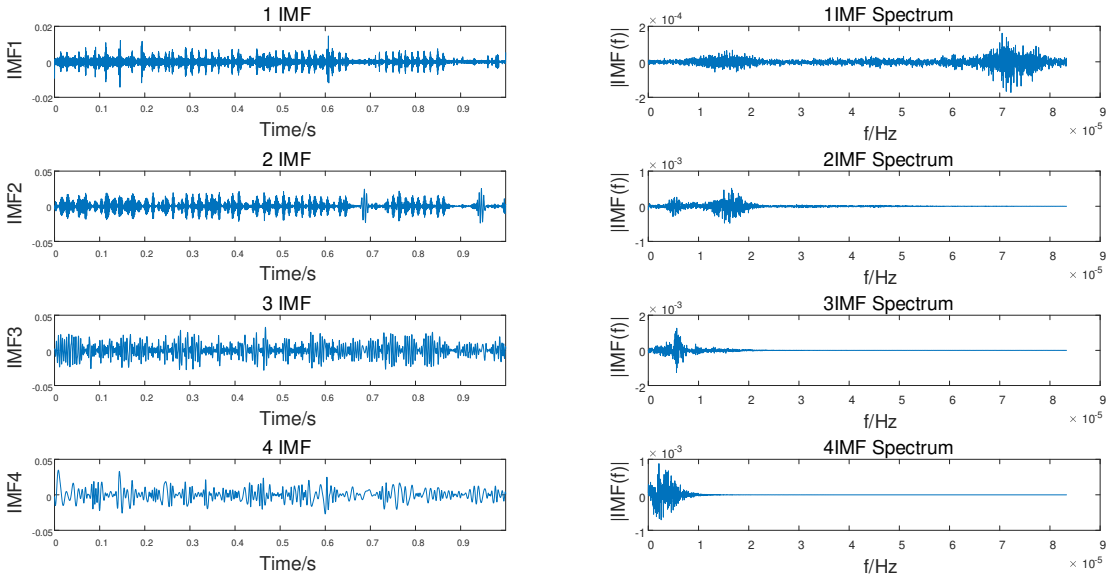
142
143
144
145

Figure 9 and 10 show the 1 to 4 IMFs of light severe sputum stasis and severe sputum stasis signals, which convey the most information of original signals.



146
147

Figure 9. 1 to 4 IMFs light severe sputum stasis



148
149

Figure 10. 1 to 4 IMFs of severe sputum stasis

150 It can be seen from figure 9 and 10 that the combination of the IMFS and spectrum results
151 are almost equal to the original signal. Moreover, according to the comparison between severe
152 sputum stasis IMFs and mild sputum stasis IMFs, the severe sputum stasis causes more
153 unregular and strong sound noise.

154 The results of the figure 9 and 10 comparing to original signals respectively demonstrate
155 that the IMFs has similar components which is similar to the original signal. In other word, all
156 the IMFs can demonstrate part information of original signal. The combination of all IMFs
157 information equal to original signal, which means the whole information can be almost kept.

158 After got the IMFs, then do the Hilbert translation for every IMFs:

$$159 \quad \hat{h}_i(t) = \frac{1}{\pi} \int_{-\infty}^{+\infty} \frac{\hat{h}_i(\tau)}{t - \tau} d\tau \quad (9)$$

160 $\hat{h}_i(t)$ is represent each IMFs, then construct analytic function:

$$161 \quad z_i(t) = h_i(t) + j\hat{h}_i(t) = a_i(t)e^{-j\varphi_i(t)} \quad (10)$$

162 After that the amplitude function can be got:

163
$$a_i(t) = \sqrt{h_i^2(t) + \hat{h}_i^2(t)} \quad (11)$$

164 The instantaneous frequency $f_i(t)$ is:

165
$$f_i(t) = \frac{1}{2\pi} \omega_i(t) \quad (12)$$

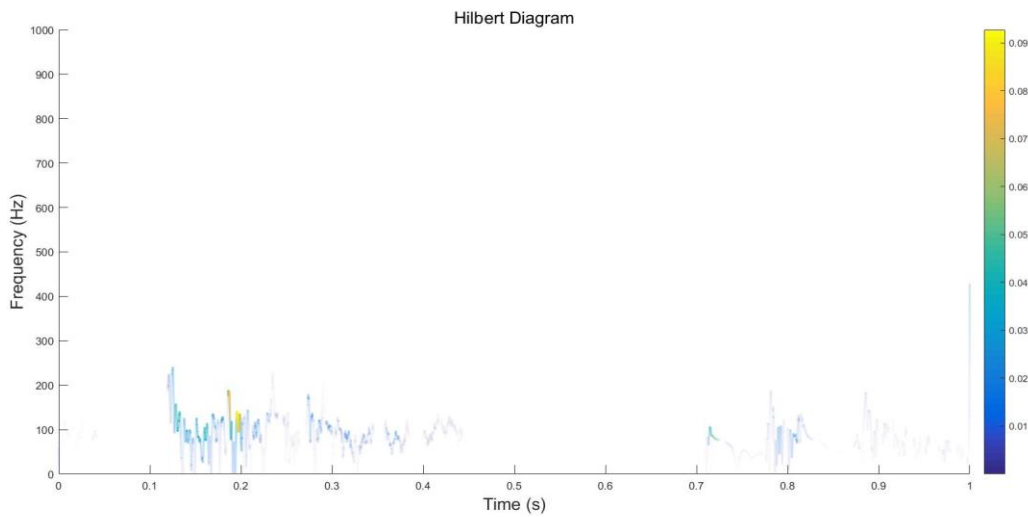
166
167 Then:

168
$$x(t) = Re \sum_{i=1}^n a_i(t) e^{-j \int \omega_i(t) dt} \quad (13)$$

169 Thus, the Hilbert Diagram can be obtained according to the function (14)

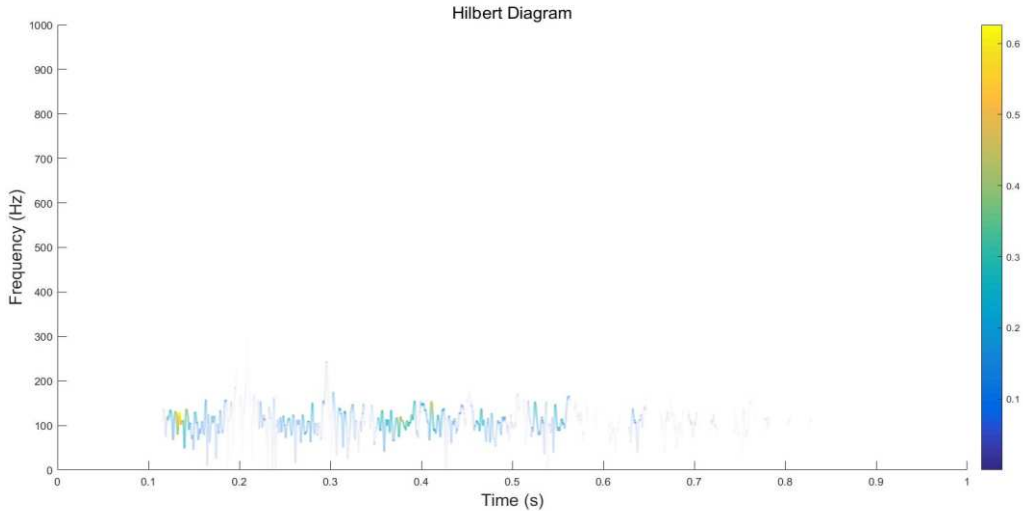
170
$$H(\omega, t) = Re \sum_{i=1}^n a_i(t) e^{-j \int \omega_i(t) dt} \quad (14)$$

171
172 The Hilbert Diagram can reflect the amplitudes of IMFs change in the whole frequency
173 band with time and frequency change.



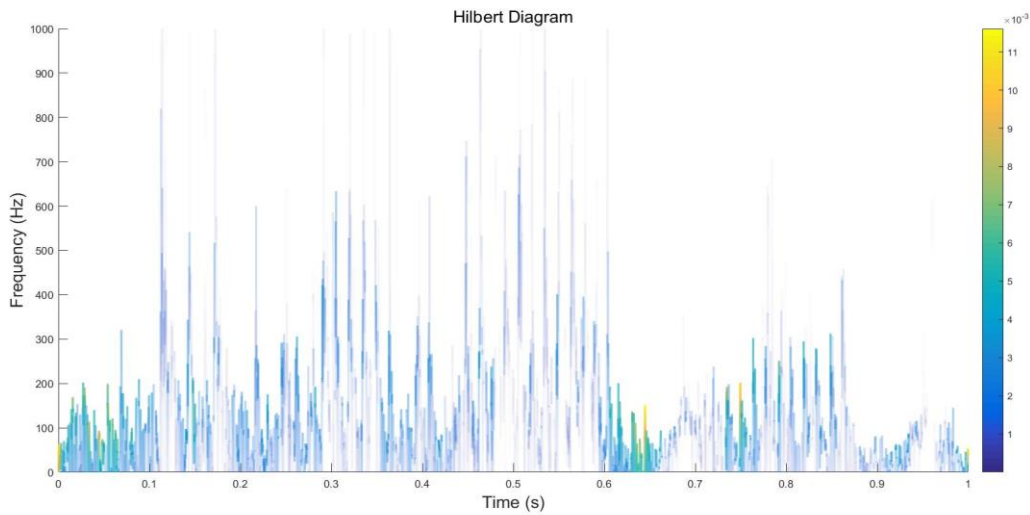
174
175

Figure 11. Hilbert Diagram of mild sputum stasis



176
177

Figure 12. Hilbert Diagram of light severe sputum stasis



178
179

Figure 13. Hilbert Diagram of severe sputum stasis

180 As shown in figure 11, 12 and 13, the Hilbert Diagram shows the IMFs frequency change
 181 characteristics with time change. The color represents different amplitude of signals. The
 182 results illustrate that the after de-noise and empirical mode decomposition, the characteristics
 183 of original signals are almost kept. From above figures, mild sputum stasis and light severe
 184 sputum stasis results shows that the frequency of this two signals frequency concentrates in 0
 185 to 200 Hz. For severe sputum stasis signal, although the frequency range is more wide than the
 186 other two signals, the high amplitude part still concentrate in 200 Hz below frequency range.

187 Wavelet Decomposition

188 Wavelet Decomposition (WD) is a signal decomposition method based on wavelet
 189 transform. The wavelet transform can be represented by the equation below:

$$190 \quad CWT_f = \int_{-\infty}^{+\infty} f(x)\overline{\varphi(x)}dx \quad (15)$$

191 In the equation (9), $\overline{\varphi(x)}$ that represent wavelet mother function is

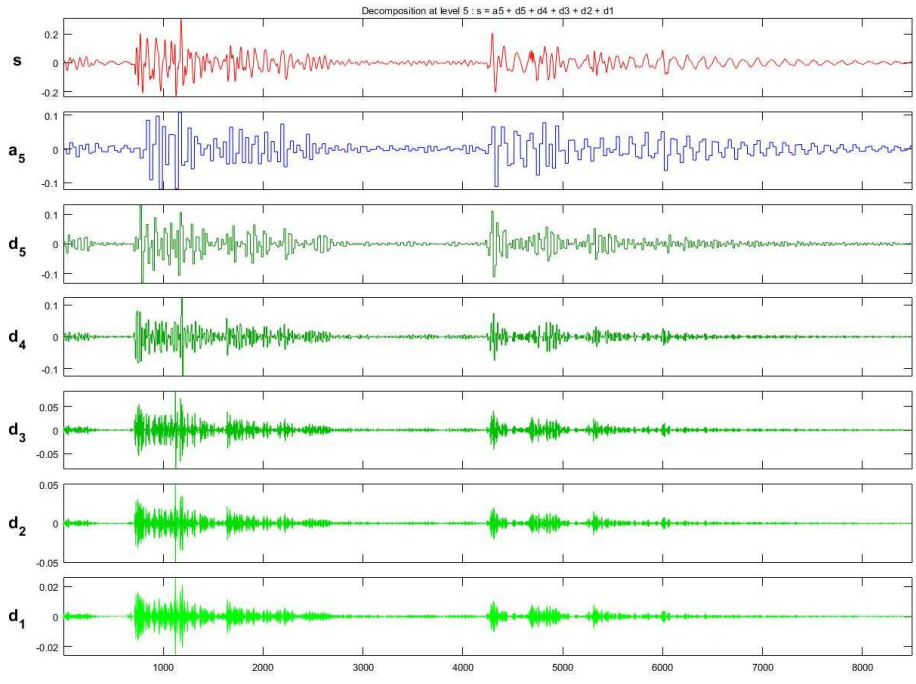
$$192 \quad \overline{\varphi(x)} = |a|^{-\frac{1}{2}}\varphi\left(\frac{x-b}{2}\right) \quad a, b \in R \quad (16)$$

193 The a is the dyadic dilation and the b represent dyadic position.

194 Equation (11) is showing the Discrete Wavelet Transform:

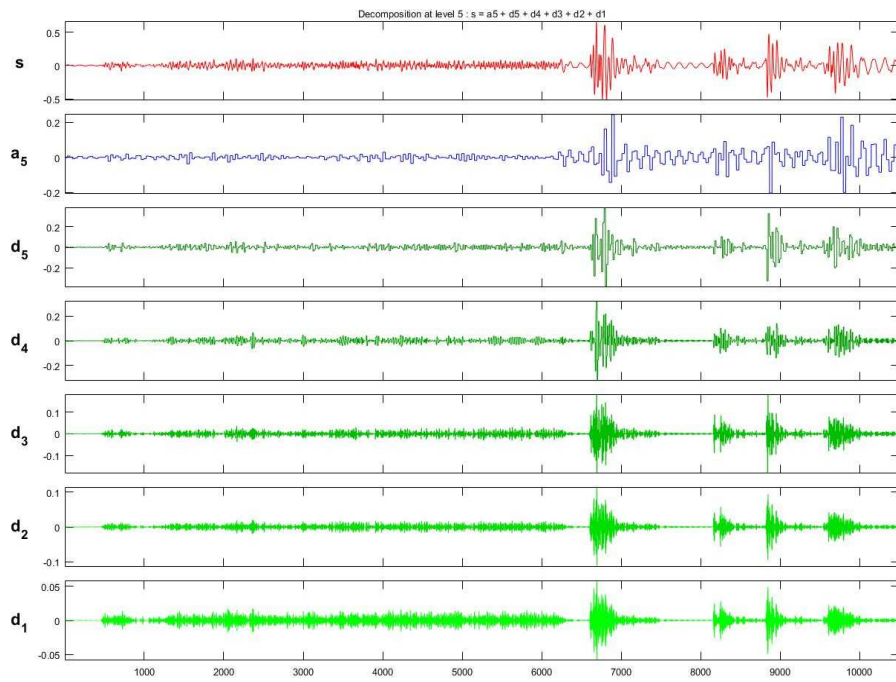
195
$$DWT_f(c, d) = \int_{-\infty}^{+\infty} f(x)\varphi_{c,d}(x)dx = a_0^{-\frac{c}{2}} \int_{-\infty}^{+\infty} f(x)\varphi\left(a_0^{-\frac{c}{2}}t - kb_0\right)dx \quad (17)$$

196 The DWT has high complexity for calculation. Then using the MALLAT algorithm to do
197 the wavelet decomposition which is using for making the calculation easier. By using multi-
198 resolution decomposition of the purpose signal, the coefficients can be obtained. [14,15]



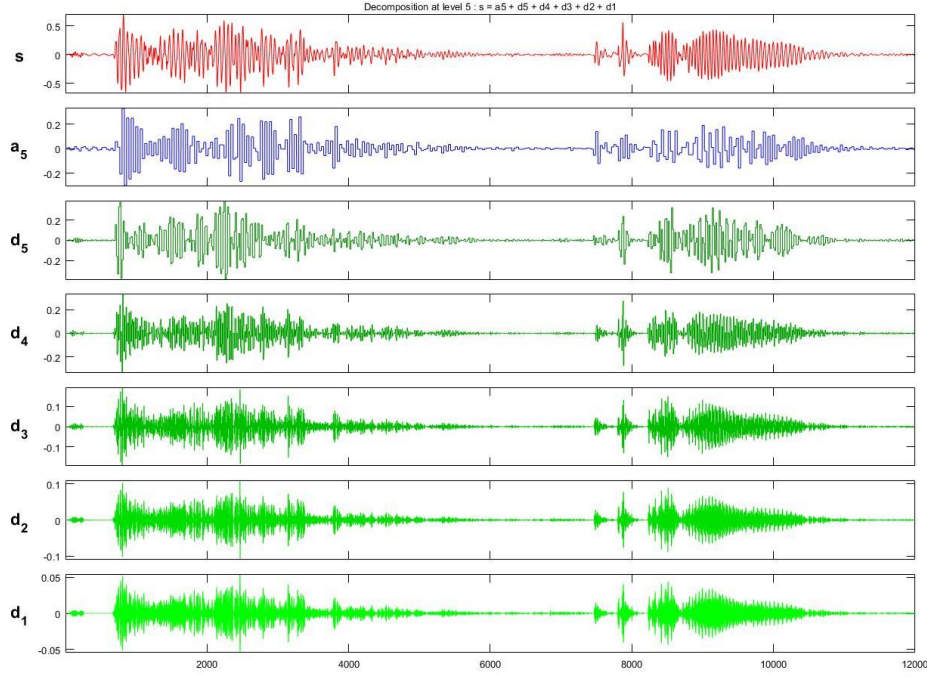
199
200

Figure 14. mild sputum stasis respiratory sound wavelet decomposition



201
202

Figure 15. slight severe sputum stasis respiratory wavelet decomposition



203
204 **Figure 16.** severe sputum stasis respiratory wavelet decomposition

205 The above figure 14 to 16 show the decomposition results of mild sputum stasis, slight
206 severe sputum stasis and severe sputum stasis sound signals.

207 The disorder of the probability distribution of a random process can be measured by
208 Shannon entropy as shown in following equation [16]

209
$$S_{WT} = \sum_i p_i \ln\left(\frac{1}{p_i}\right) \quad (18)$$

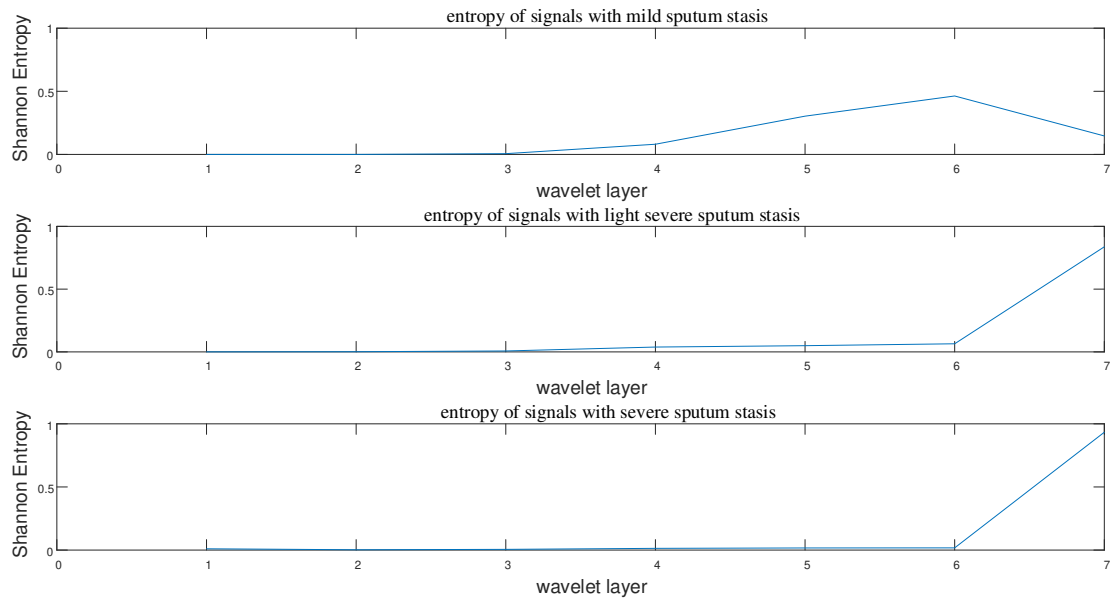
210 p_i shows in the equation represent the probability of a random process.

211 If the p_i can be represented by Relative Wavelet Energy (RWE), this entropy can define the
212 disorder of the relative wavelet energy distribution. [17] The relative wavelet energy can be
213 calculated by:

214
$$RWE_i = \frac{WEN_i}{WEN_{total}} \quad (19)$$

215 The WEN_i in equation (13) is layer I wavelet energy and WEN_{total} is the total wavelet
216 energy.

217 Thus, the Shannon entropy of relative wavelet energy of mild, slight severe and severe
218 sputum stasis is showing in figure 17.



219

220

Figure 17. Shannon entropy of mild, slight severe and severe sputum stasis

221

222

223

224

225

226

227

As shown in the result, the RWE Shannon entropies of light severe and severe sputum stasis signal on the seventh wavelet layer are more than 85%. Thus, the most information of the signal is concentrated on layer 7. However, the mild sputum stasis signal has different information distribution. Thus, when it comes to signal analysis, the different distribution method can lead to hard to define the feature vector of the signal. In the contrast, the EMD method information distribution is concentrate on first 1 to 4 IMF, which has stable distribution.

228

Conclusion

229

230

231

232

233

234

235

236

237

238

239

In conclusion, this article is using spectrum subtraction de-noise method process three kinds of signals, mild sputum stasis, slight severe sputum stasis and severe sputum stasis sound signals. The spectral subtraction de-noise method has efficient effect in preprocessing respiratory sound. After preprocess, results of the three kinds of signals are decomposed by EMD and WD separately. The EMD results are transformed by Hilbert transformation function and the Hilbert diagrams showing the results that all the information of original signals is keeping well and concentrating in 200 Hz frequency range for EMD method. Results of WD were processed with Shannon entropy of RWE. In the end, the information of original signals over 85% is kept in layer 7 of wavelet transformation for light severe and severe signals, which cannot be analyzed well. It turns out that the EMD has better efficiency in preprocessing signals than WD.

240

241

242

243

244

Funding: This paper is supported by the Open Research Project of the State Key Laboratory of Media Convergence and Communication, Communication University of China, China (No. SKLMCC2020KF002), the fundamental research funds for central public welfare research institutes, National Key Research and Development Project (No. 2019YFC0121700) and Grant (No.2019M660392) of China Postdoctoral Science Foundation.

245

Reference

246

247

1. Fei Meng, Yan Shi, Na Wang, Maolin Cai, Zujing Luo, 'Detection of Respiratory Sounds Based on Wavelet Coefficients and Machine Learning', 2020, [J], Journal of Robotics & Machine Learning

- 248 2. Z. Moussavi, "Fundamentals of respiratory sounds and analysis," Synth. Lectures Biomed. Eng., vol.
249 1, no. 1, pp. 1–68, Jan. 2006.
- 250 3. S. Reichert, R. Gass, A. Hajjam, C. Brandt, E. Nguyen, K. Baldassari, and E. Andrès, "The ASAP project:
251 A first step to an auscultation's school creation," Respiratory Med. CME, vol. 2, no. 1, pp. 7–14, 2009
- 252 4. M. Sarkar, I. Madabhavi, N. Niranjana, M. Dogra, Auscultation of the respiratory system, Ann. Thorac.
253 Med. 10 (3) (2015) 158–168
- 254 5. E. Saatci, A. Akan, Heart sound reduction in lung sounds by spectrogram, in: IFMBE Proc, Vol. 11, 2005,
255 pp. 1727-1983. No.1.
- 256 6. L.J. Hadjileontiadis, Empirical Mode Decomposition and Fractal Dimension Filter. IEEE ENG. Med.
257 Biol. Mag. 26 (1) (2007) 30.
- 258 7. Emmanouilidou, D., McCollum, E.D., Park, D.E., Elhilali, M. 'Adaptive Noise Suppression of Pediatric
259 Lung Auscultations with Real Applications to Noisy Clinical Settings in Developing Countries'(2015)
260 IEEE Transactions on Biomedical Engineering, 62(9), 7084596, pp.2279-2288.
- 261 8. Haider Nishi Shahnaj. Respiratory sound denoising using Empirical Mode Decomposition, Hurst
262 analysis and Spectral Subtraction[J]. Biomedical Signal Processing and Control, 2021, 64 : 102313.
- 263 9. Huang NE, Shen Z, Long SR, Wu MC, Shih HH, Zheng Q, Yen N-C, Tung C-C, Liu HH (1998) The
264 empirical mode decomposition and the Hilbert spectrum for nonlinear and non-stationary time series
265 analysis. R Soc 454:903–995
- 266 10. YANG H F, CHEN Y P P. Hybrid deep learning and empirical mode decomposition model for time
267 series applications[J]. Expert Systems with Applications, 2019, 120(1): 128-138.
- 268 11. BOUNY L E, KHALIL M, ADIB A. Performance analysis of ECG signal denoising methods in
269 transform domain[C]. International Conference on Intelligent Systems & Computer Vision, 2018 :1-8 .
- 270 12. Hossain I, Moussavi Z. An overview of heart-noise reduction of lung sound using wavelet transform
271 based filter. In Proceedings of the 25th Annual International Conference of the IEEE Engineering in
272 Medicine and Biology Society. 2003, 1: 458-461.
- 273 13. A. Kandaswamy, C. S. Kumar, R. P. Ramanathan, S. Jayaraman, and N. Malmurugan, "Neural
274 classification of lung sounds using wavelet coefficients," Comput. Biol. Med., vol. 34, no. 6, pp. 523–537,
275 Sep. 2004
- 276 14. S. Mallat, A Wavelet Tour of Signal Processing. New York, NY, USA: Academic, 1999.
- 277 15. S. G. Mallat, "A theory for multiresolution signal decomposition: The wavelet representation," IEEE
278 Trans. Pattern Anal. Mach. Intell., vol. 11, no. 7, pp. 674–693, Jul. 1989.
- 279 16. C. E. Shannon, "A mathematical theory of communication," ACM SIGMOBILE Mobile Comput.
280 Commun. Rev., vol. 5, no. 1, pp. 3–55, 2001.
- 281 17. R. X. A. Pramono, S. A. Imtiaz, and E. Rodriguez-Villegas, "Evaluation of features for classification of
282 wheezes and normal respiratory sounds," PLoS ONE, vol. 14, no. 3, Mar. 2019, Art. no. e0213659.